

RESEARCH

Study on Fingertip Slippage using FE Model for Developing Human-Like Tactile Sensor

Zhongkui Wang*, Damith Suresh Chathuranga and Shinichi Hirai

Abstract

Slippage on the fingertips is an important phenomenon that occurs constantly in our daily life and it is indispensable in human tactile sensation. However, the mechanism of slippage, especially the incipient slippage, which occurs prior to overall slippage, has not been fully understood and has not yet been studied frequently. Therefore in this paper, fingertip slippage is studied using finite element (FE) simulations. 2D and 3D fingertip models were generated based on magnetic resonance (MR) images. The models consist of layered structures denoted by skin, subcutaneous tissue, and distal phalanx. In 2D model, the skin layer is further divided into epidermis and dermis layers and the microstructures of the intermediate and limiting ridges, and fingerprints were included. The overall behaviors during pushing and sliding motion were studied using 3D model, and the detailed responses of different mechanoreceptors located in human fingertip were investigated with the 2D model. We found that mechanoreceptors of fast-adapting type I (FA-I) and slow-adapting type I (SA-I) are sensitive to the micro vibrations occurring during slippage and they can capture incipient slippage as well as overall slippage. The effects of phalanx geometry, fingerprint, and friction coefficient were also investigated through simulations. An artificial fingertip mimicking human fingertip geometry was constructed and pushing-and-sliding tests were conducted to validate some simulation results.

Keywords: fingertip; slippage; incipient; tactile; finite element

Background

Humans constantly use their hands and fingertips to explore and interact with the physical world. We can dexterously grasp and manipulate an object with minimal efforts thanks to the excellent tactile system located within our fingertips. Slippage, especially incipient slippage which occurs prior to the overall slippage, is believed to be an important phenomenon during object grasping and manipulation [1, 2]. Human fingers can detect the slippage and increase the gripping forces or change the gripping posture to avoid undesirable manipulation failures [1]. To mimic or reproduce such abilities of human fingertips, the mechanism behind slippage perception needs to be clarified.

Researches on human tactile perception have been carried out for more than three decades. Johansson and Vallbo reported that there are about 17,000 mechanoreceptors in human hand to perceive tactile sensation [3]. Based on the locations and sensitivities, they were further divided into four types: fast-adapting type I (FA-I, Meissner endings),

slow-adapting type I (SA-I, Merkel endings), fast-adapting type II (FA-II, Pacini endings), and slow-adapting type II (SA-II, Ruffini-like endings) [4]. Neural responses of SA-I to bar, edge, and grating indentations were experimentally measured with monkey fingertips [5], and a continuum mechanical model was proposed to fit the neural response [6]. It was concluded that the maximum compressive strain is a close approximation of SA-I response. Since then, various models, such as a “waterbed” model [7], 2D FE models [8, 9], and 3D FE models [10, 11], were proposed to investigate the mechanics of tactile sensation by fitting the SA-I neural response with various mechanical measures. Researchers agreed that the strain energy density (SED) is the best mechanical measure to translate the SA-I neural response. Recently, a multi-level model was proposed in [12] to complete the loop from external stimuli to SED calculation, to membrane current transformation, and finally to neural spike time generation. Basically, the above-mentioned FE models have detailed structure with approximated geometries of the fingertips. Static indentation simulations were usually performed and mechanical measures calculated in the locations of receptors were fitted

*Correspondence: wangzk@fc.ritsumei.ac.jp

Department of Robotics, Ritsumeikan University, Noji-Higashi 1-1-1, 525-8577 Kusatsu, Japan

Full list of author information is available at the end of the article

to neural responses. Unfortunately, simulation and evaluation of slippage has not been addressed so far.

On the other hand, researches on slippage date back to the 80s. A series of experiments were performed by Johansson and Westling to study the balance between grip and load forces while subjects lift small objects [13]. It was found that the balance between these two forces is adapted to the friction between the object and the fingertip providing a relatively small safety margin to prevent slips. The time latency between the onset slippage and the appearance of adjustment is about 60–80 ms, which indicates that the underlying neural mechanism operated locally and automatically. Further in [1], the neural afferent responses during grasping were recorded, and the mechanoreceptors of FA-I, FA-II, and SA-I were found to be sensitive to slippage. Specifically, it was reported that the “localized slip responses” (*i.e.* incipient slippage) were mainly detected by FA-I and SA-I receptors, and the “initial responses” mostly appeared in the FA-I receptors. Based on these findings, various tactile sensors for detecting slippage were proposed with varying degrees of success. Howe and Cutkosky proposed a method to detect slippage by sensing the micro-vibration happening near the contact area [14]. This sensor consists of a rubber skin layer, a foam rubber layer, and a hard plastic core to mimic the human fingertip structure. One accelerometer was mounted on the inner surface of the skin and placed near the contact area. The slippage was revealed by the large vibration appeared in acceleration measurements. This sensor was then improved to detect incipient slippage by adding vibrating “nib” to cover the skin surface and adding another side accelerometer far away from the contact area [15]. The authors claimed that the sensor can capture the incipient slippage, but the acceleration peak is believed to be a combination of incipient slip signal and acceleration signal due to the increasing of gripping force. Actually, the incipient slippage was not clearly recognized by the sensor.

Methods based on measurements of stress and stress rate were also proposed using piezoelectric polymer film [16] and PVDF film [17, 18]. Additionally, methods based on displacement measurement were presented using either an imaging system [19] or an optic fiber array [20]. In our previous work [21], a human-like tactile sensor was proposed by embedding force sensors and accelerometers into a biomimetic layer structured fingertip as shown in Fig. 1. This tactile sensor was successfully applied to discriminate different wood textures, but has difficulties to detect slippage, especially the incipient slippage. Above-mentioned tactile sensors have attempted to use different mechanical measures, such as strain or displacement, stress or force, and acceleration, to translate how human fingertip perceive slippage. Measuring strain or displacement on contact area is a straightforward way to capture incipient slippage. However, it often requires an external imaging sensor [19] or

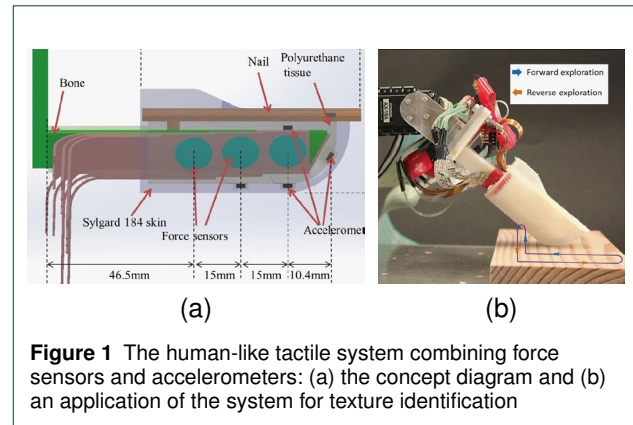


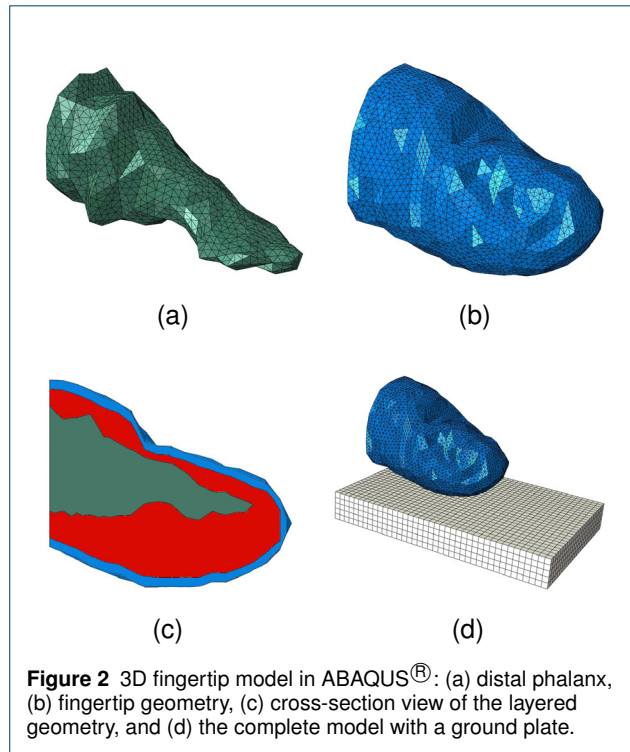
Figure 1 The human-like tactile system combining force sensors and accelerometers: (a) the concept diagram and (b) an application of the system for texture identification

a relatively complicated measuring system [20]. Measuring stress or force inside the fingertip captures the low-frequency signals but misses the high-frequency signals. Measuring acceleration, on the other hand, can capture the high-frequency signals but it is vulnerable to environment vibrations. Combining different sensors together is one way to improve the performance, but how to arrange the locations of the sensors to optimize the performance raises a question. Besides, there are still many open questions regarding slippage, such as, how the human fingertip perceive slippage, how the fingertip structure (*e.g.* the geometry of the distal phalanx or fingerprint) affects the slippage perception, how the time latency differs among different slipping conditions, and so on. This again encourages us to investigate the mechanism behind fingertip slippage, especially, the incipient slippage.

Due to the difficulties of experimentally monitoring mechanical responses inside human fingertip, in this paper, we propose FE models to simulate and study these responses and understand the mechanism of fingertip slippage. 3D and 2D FE models of an index fingertip with detailed anatomical geometries are introduced in the next section, followed by the simulation results and discussions. Then, an artificial fingertip model was proposed to validate some of simulation results. Finally, the paper is concluded with some suggestions of future works.

Methods

MR images of an index finger were taken with a 25-year-young subject with no history of finger diseases [22]. Through image processing, the boundaries of distal phalanx and finger surface were generated and 3D geometries of both parts, as shown in Figs. 2a and 2b, were reconstructed by connecting the boundary nodes. The internal boundary of skin was generated by scaling down the finger surface by 1 mm to approximate the thickness of the skin. Accordingly, the fingertip was separated into three regions denoted by skin, subcutaneous tissue, and distal phalanx. The geometries of these regions were then imported into FE package ABAQUS[®] for further processing.

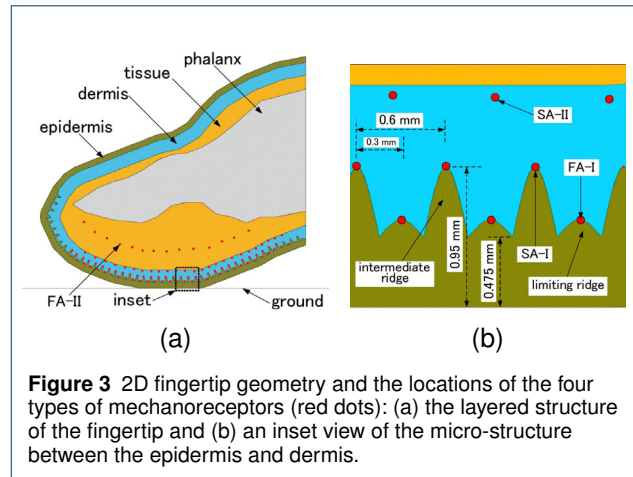


3D fingertip model

A cross-section view of the fingertip is shown in Fig. 2c. In ABAQUS[®], the connections between two tissue layers were defined as “tie” constraints. A ground plate was created underneath the fingertip (Fig. 2d) to provide support and activate the pushing-and-sliding simulation. The parts of distal phalanx, tissue, and skin were meshed with a 4-node linear tetrahedron element, and the ground plate was meshed with an 8-node linear brick element. The model consists of a total of 33,957 nodes and 130,492 elements. During simulations, the distal phalanx is fixed in space and the ground plate is firstly displaced upward to deform the fingertip in 0.5s with a pushing velocity of 4mm/s. Then, the ground plate slides backward (fingertip slides forward) with a velocity of 5 mm/s until overall slippage happened. The interactions between the ground plate and the skin surface were defined as normal and tangential behaviors using the penalty method. The friction coefficient was set as 0.6.

2D fingertip model

To investigate the effects of micro-structures and locate the four types of mechanoreceptors inside fingertip, 2D FE model was developed. The 2D geometries, as shown in Fig. 3a, were generated from the projection of the 3D geometries. The skin consisting of epidermis and dermis layers was assumed to have a thickness of 1.5mm [10]. The micro-structures of the intermediate and limiting ridges in between the epidermis and dermis are detailed in Fig. 3b. The dimensions of the ridges were referred from literature



[23]. The FA-I receptors were assumed to be located at the top of the limiting ridges, the SA-I receptors were located at the top of the intermediate ridges, and the SA-II receptors were located near the border between the dermis and the tissue layers, as shown in Fig. 3b. The FA-II receptors were assumed to be located at a depth of 3mm from the surface of the skin, and the locations are shown in Fig. 3a.

To investigate the effects of different distal phalanx geometries and fingerprint, 2D FE models with a flattened phalanx, a scaled phalanx, and fingerprint structure were proposed as well (Fig. 4). The flattened phalanx was generated by flattening the phalanx bottom surface and make

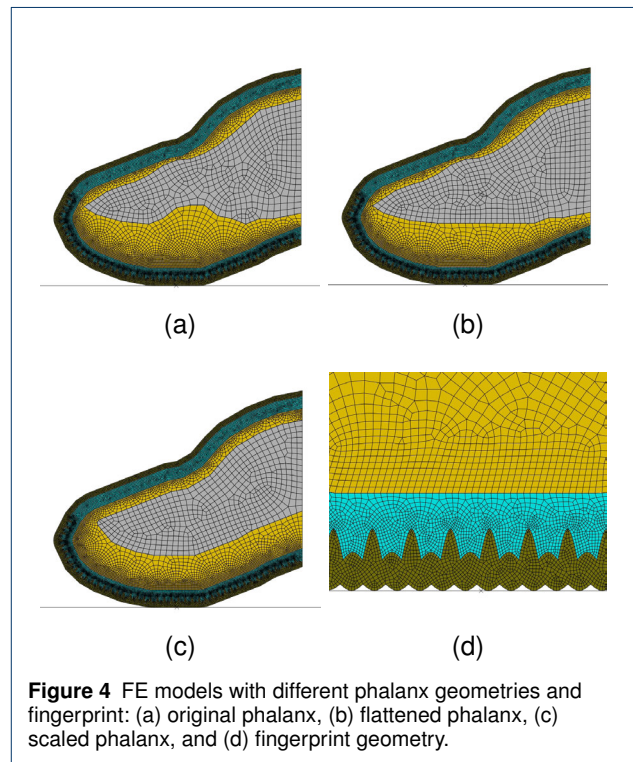


Table 1 Material properties of the tissue layers

Tissue Layer	Young's Modulus	Poisson's Ratio	Tissue Density
Phalanx	1.5×10^9 Pa	0.3	449 Kg/m ³
Tissue	3.4×10^4 Pa	0.48	1000 Kg/m ³
Dermis	8.0×10^4 Pa	0.48	1000 Kg/m ³
Epidermis	1.36×10^5 Pa	0.48	1000 Kg/m ³

the bottom parallel with the ground plate (Fig. 4b). The scaled phalanx was generated by scaling the skin surface inward so that the tissue thickness between skin and phalanx is uniform (Fig. 4c). The fingerprints were modeled as continuous ripples (Fig. 4d) and the dimension of the ripple is referenced from [24]. In 2D FE models, the ground was modeled as an analytical rigid shell and all parts were meshed with 4-node bilinear quadrilateral element. Other conditions are same as 3D model. During simulations, the pushing and sliding velocities of the ground plate were set to 1.5 mm/s and 3 mm/s respectively and finally the ground plate achieved a vertical displacement (pushing) of 1.5 mm and a horizontal displacement (sliding) of 6 mm, which is long enough to generate overall slippage. All simulations were carried out using implicit dynamic analysis, and the geometrical nonlinearity was turned off. All tissue layers were modeled as linear elastic materials, and the physical properties of tissue layers were referenced from [24] and are given in Table 1.

Results and discussions

Results and discussions of the 3D model

Figure 5 shows the simulation results of slippage on the skin surface. The slippage was defined as the relative motion of the contact area on skin to the ground plate, as shown by different colors. We found that the nodes on contact area were sticking with the ground plate from time 0.5 s (the end of pushing) to about 0.9 s and there is no or very little relative motion on the contact area, as shown in Figs. 5a and 5b. From time 0.9 s, some peripheral nodes started to slip with small relative motion, as shown in Fig. 5b and 5c. This can be considered as incipient slippage or localized slippage. After that moment, the relative motion spreads from the periphery to the center of the contact area until time 1.1 s (Fig. 5d) when the overall slippage happened. After overall slippage, the relative motion of the contact area was increasing uniformly (Figs. 5e and 5f). At the end of the simulation (Fig. 5f), we can see that the relative motions on peripheral nodes are larger than those on the center area. Figure 5 clearly showed the incipient slippage and agrees well with the consensus on incipient slippage, which occurs firstly at the peripheral area and spreads towards the center area until overall slippage. From Fig. 5, we found that there is about 200 ms (from 0.9 s to 1.1 s) time latency between incipient and overall slippages, within which we

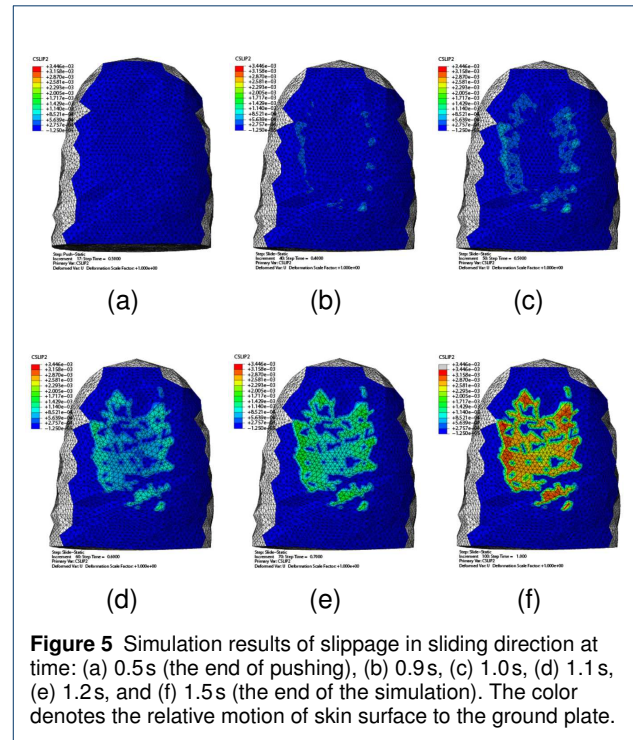
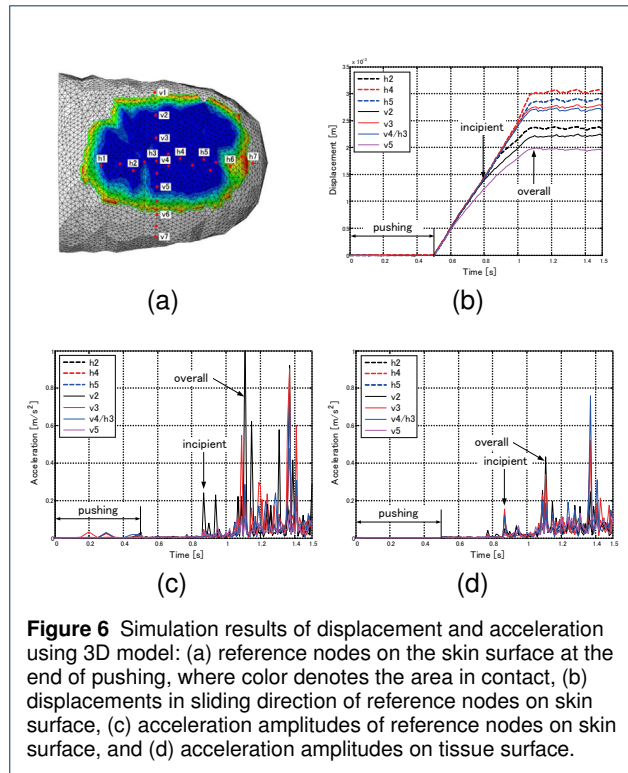


Figure 5 Simulation results of slippage in sliding direction at time: (a) 0.5s (the end of pushing), (b) 0.9s, (c) 1.0s, (d) 1.1s, (e) 1.2s, and (f) 1.5s (the end of the simulation). The color denotes the relative motion of skin surface to the ground plate.

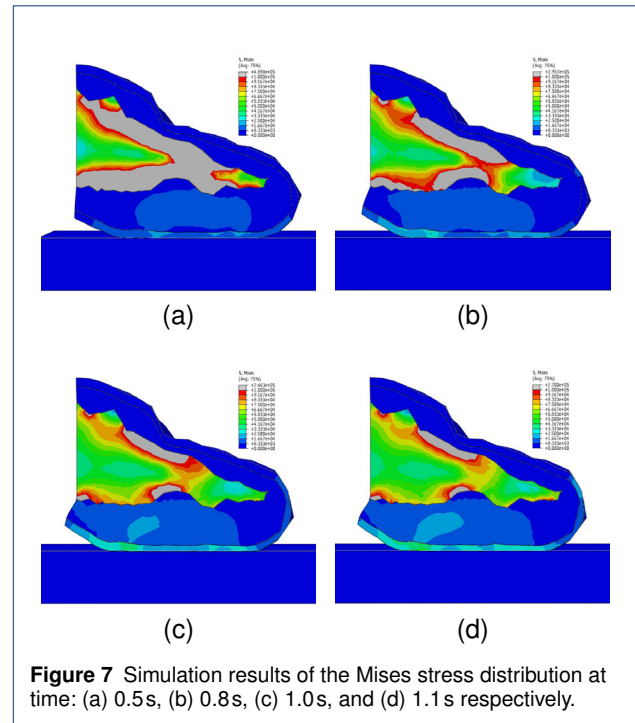
can increase gripping force or change gripping strategy in order to avoid slippage.

To quantitatively investigate the mechanical measures generated on or inside the fingertip, some reference nodes were defined on both skin and tissue surfaces in horizontal (h1 through h7) and vertical (v1 through v7) directions. An example was shown in Fig. 6a for skin surface at the end of pushing. As we can see that nodes h2 through h5 and v2 through v5 were actually in contact with the ground plate and simulation results on these nodes were focused in the following analysis. Figure 5b shows displacement results in the sliding direction on skin surface. We found that the contact nodes were firstly moving together with the ground plate and having the same velocity (the linear slope) with the ground. After a certain time, some nodes started to give away and move apart from the slope. This moment is considered as the start of incipient slippage. The moment when all contact nodes gave away is considered as the start of overall slippage. Based on Fig. 6b, we know that the incipient slippage started at about 0.8 s (indicated by the arrow), and the overall slippage started at about 1.1 s. Therefore, we would have a latency of about 300 ms between incipient and overall slippages if we could accurately monitor the movements of all contact nodes. Note that the latency seen from Fig. 5 was about 200 ms because the color scale is set large and very small slippage was not visible. Measuring movements on contact area is a straightforward and effective way to detect incipient slippage. However, it is normally a challenging task since it requires real-time motion



capture and image processing with high resolution. Figures 6c and 7d show the acceleration responses of the reference nodes on both skin and tissue surfaces. We found a large peak at time 1.11 s which agreed with Fig. 5 as the sign of overall slippage. Before this moment, we also found two large peaks (0.87 s and 0.94 s) on the skin surface and one large peak (0.87 s) on the tissue surface. These peaks can be considered as a sign of incipient slippage. Therefore, we could have a time latency of 240 ms based on the acceleration responses. Comparing Fig. 6c and Fig. 7d, we found that the peak amplitudes on tissue surface are smaller than those on skin surface. This tells us that the layer of epidermis works as a damper reducing the acceleration signals. Based on Fig. 6, we can conclude that both incipient and overall slippages were clearly showed in acceleration signals on both skin and tissue (under-skin) surfaces.

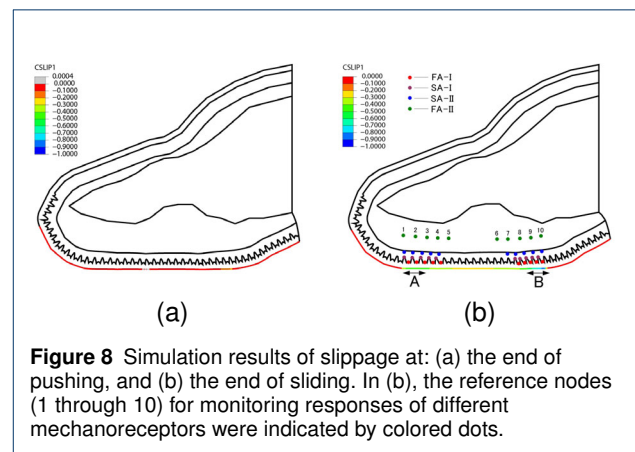
Figure 7 shows the Mises stress distribution inside the fingertip with a cross-section view. We found that the distal phalanx was under much larger stress comparing with soft tissues, and the stress was decreasing during sliding. Large stresses were concentrated in the concave area and the area opposite to it. After time 1.1 s, the stress distribution barely changed, which means the stress state achieved a balance after overall slippage. During sliding, stresses inside tissue and skin were increased due to the continuously increased deformation of these tissues. We found that large stresses distributed peripherally on the contact area of skin layer. This is surprising since the center area actually de-



forms more and larger stress is usually expected. We believe that this may be caused by the distal phalanx geometry, on which a concave area is located above the contact center. The effect of distal phalanx geometry on slippage was addressed in the next Section. Unfortunately, we could not find any clear sign from the stress distribution to indicate the moments of slippages.

Results and discussions of 2D model

Simulations of 1 s pushing and 3 s sliding using 2D FE models were performed and mechanical responses at the locations of different mechanoreceptors (Fig. 3) were presented in this section.



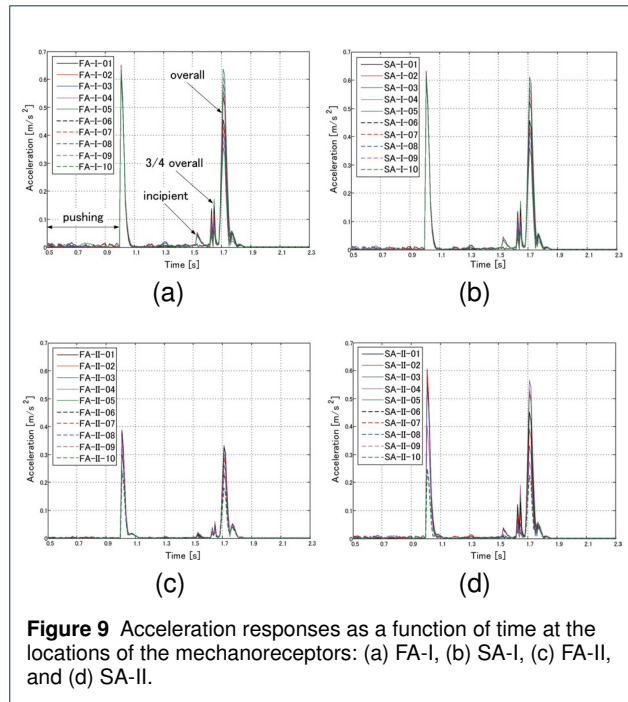
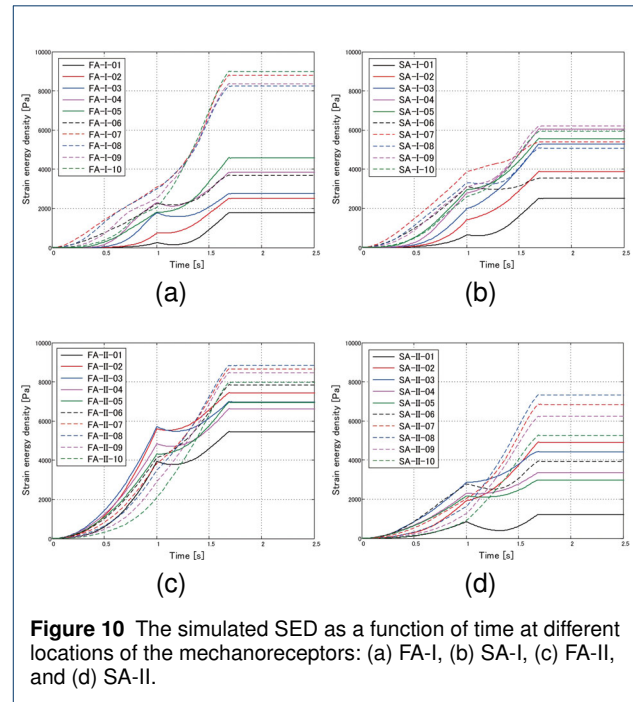


Figure 8 shows the simulation results of slippage on the skin surface with red indicating no slipping and blue indicating a slipping displacement of 1 mm. Similar to Fig. 5, we found that the slipping occurs first at the peripheral area (areas A and B in Fig. 8b) and then spreads towards center area at the end of sliding. Therefore, 10 reference nodes were selected around the peripheral areas for each type of mechanoreceptors, as shown in Fig. 8b, to study the relationship between the mechanical responses at different mechanoreceptors and the slippages.

Figure 9 shows the acceleration responses as a function of time at the locations of four types of mechanoreceptors. We found that the first peak in acceleration was at the moment of the motion transition from pushing to sliding. While during sliding, we found four distinct peaks with increasing peak magnitudes. The first one at 1.53 s could be considered as the start of incipient slippage. Although some fluctuations indicating micro-slipping occurred before this moment, these fluctuations could be filtered out as environmental noises. The second and third peaks were very close and appeared at time 1.63 s and 1.65 s, respectively. These peaks could be considered as the moment where 3/4 of the contact area had slipped. In [1], the authors found that not until approximately 3/4 of the contact area had slipped did an overall slip occur. If compensations, such as increased grip force and changed grip gesture, could not be triggered before this moment, the overall slipping would be inevitable. Figure 9 suggests a time latency of more than 100 ms (from 1.53 s to 1.63 s or 1.65 s) for the compensation adjustments. Finally, the last peak that appeared at 1.71 s denoted the overall slippage. Figure 9 also



shows that receptors FA-I and SA-I had more pronounced responses compared with the other two types of receptors. This result was consistent with the findings in [1].

Researchers have agreed that the SED is the best mechanical measure for approximating neural signals during edge enhancement indentation. Therefore, we plotted the SED as a function of time at the locations of the different receptors in Fig. 10. During pushing, the SED was quickly increased, and during sliding, the SED was first increased and then remained constant after overall slippage. In most of the receptors (FA-I, FA-II, and SA-II), the SED in area B (indicated by dotted lines) was clearly larger than the SED in area A (indicated by solid lines). Figure 10 suggested that the SED might be able to capture the phase changes, such as phase changes from pushing to sliding and from incipient to overall slippage, but this could only be done after the phase changed. Therefore, we can conclude that the mechanical measurement of the SED does not provide any insight for the detection of incipient slippage and cannot be used to prevent slipping.

Effects of distal phalanx geometry

Figures 11 and 12 show simulation results of acceleration responses at receptors FA-I and SA-I using flattened and scaled phalanges. We found that the second and third peaks, which appeared in Fig. 9 and denoted the 3/4 overall slippage, did not appear with using flattened phalanx (Fig. 11). While using scaled phalanx, there seems to be a second peak before the overall slippage, but it is too close to the last peak and it is hard to separate them from one another.

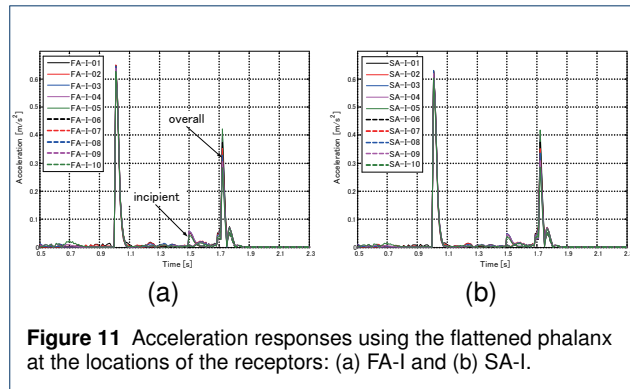
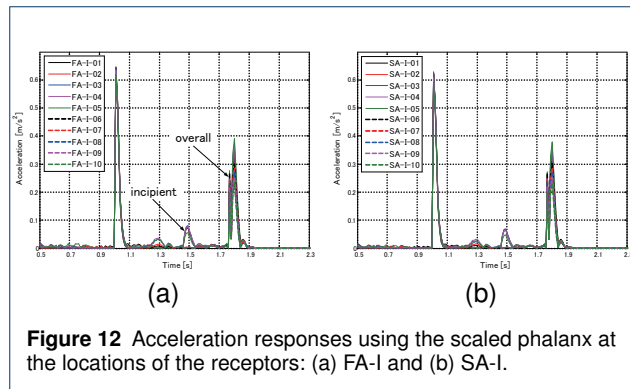


Table 2 Incipient and overall slippage moments and time latencies using different phalanx geometries

Phalanx	Incipient	Overall	Latency
Original	1.53s	1.71s	180ms
Flattened	1.50s	1.72s	220ms
Scaled	1.48s	1.77s	290ms

Effects of fingerprint

Fingerprint was commonly used for human identification and was reported to be important for texture recognition [25]. In [23], the authors claimed that the fingerprint may not directly affect SA-I mechanoreceptor response based on simulation results of static indentation. However, the effect of fingerprint on the perception of slippage has not been addressed so far. To this end, 2D FE model with fingerprints was proposed in Fig. 4d and simulation results of pushing-and-sliding motion with different geometries of phalanx were shown in Figs. 13 through 15. We found that the fingerprints introduced noise to the acceleration response at the locations of FA-I and SA-I receptors and made it impossible to identify the incipient slippage. The overall slippage can also be easily identified with fingerprint. If we compare the results with different phalanx geometries, we found that the flattened phalanx yields strong peak for recognizing overall slippage and the scaled phalanx results in strong vibrations after overall slippage. The reason why these behaviors happened remains undiscovered and it will be investigated in our future work.



Effects of friction coefficient

Figure 16 shows simulation results with different friction coefficients between the skin surface and ground plate. The original concaved phalanx was used in these simulations. Similar results with flattened and scaled phalanges were not shown in this paper. From Fig. 16, we found that the occurrence of slippage was postponed along with the increase of friction coefficient. The relationships between friction coefficient and the moments of slippages and time latencies were shown in Fig. 17. We can see that the occurrence moments for both incipient and overall slippages are linearly

Therefore, we considered the second peak as the sign of overall slippage (Fig. 12). The peak amplitudes of the incipient and overall slippage are different as well. We found that the peak amplitude indicated incipient slippage has a largest value (around 0.07 m/s^2) with using scaled phalanx, followed by the flattened phalanx (around 0.058 m/s^2), and the original concaved phalanx has the smallest peak value (around 0.054 m/s^2). However, the order is reversed when we compared the peaks indicated overall slippages, where original concaved phalanx has a value of 0.637 m/s^2 , flattened phalanx has a value of 0.423 m/s^2 , and the scaled phalanx has a value of 0.275 m/s^2 respectively. We also found that the incipient and overall slippage moments were affected by the phalanx geometries. As listed in Table 2, incipient slippages appeared earlier and overall slippage occurred later using flattened and scaled phalanges comparing with original concaved phalanx. Therefore, it results in longer time latencies using flattened and scaled phalanges. Based on the above results, it seems that the scaled phalanx provides more clear sign of incipient slippage and longer time latency for adjustments. However, only the original concaved phalanx shows the sign of 3/4 overall slippage, which provides a second chance for starting the adjustment if the first chance (incipient sign) was missing. This is probably the reason why human fingertips have robust performance on grasping and manipulation.

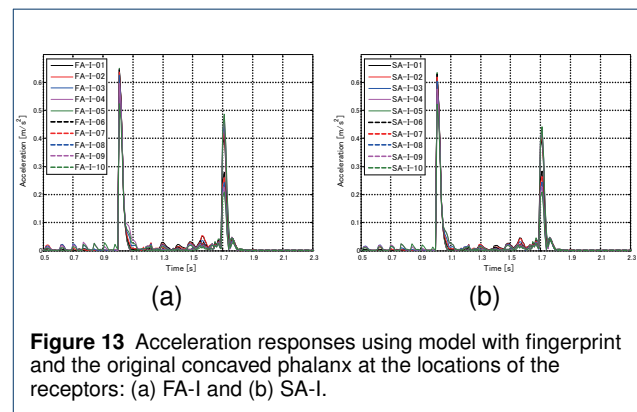
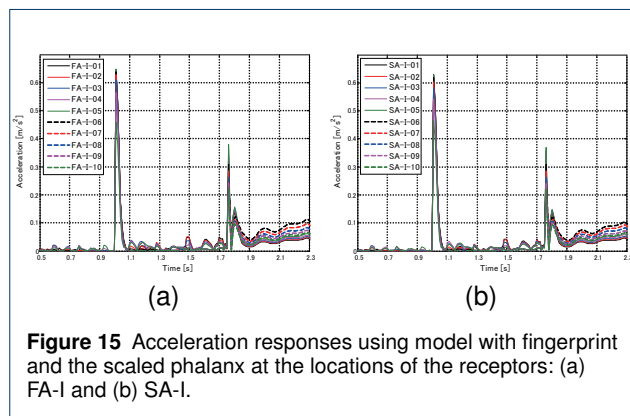
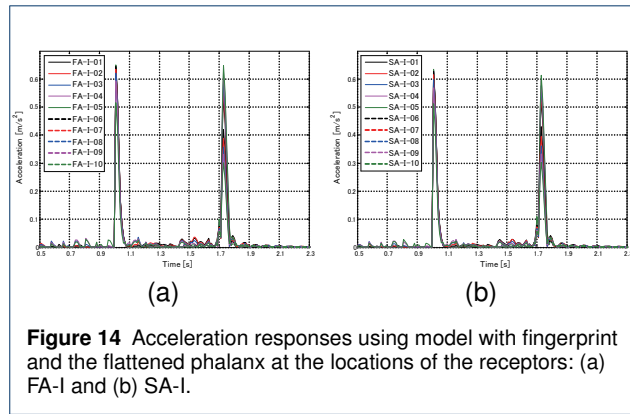


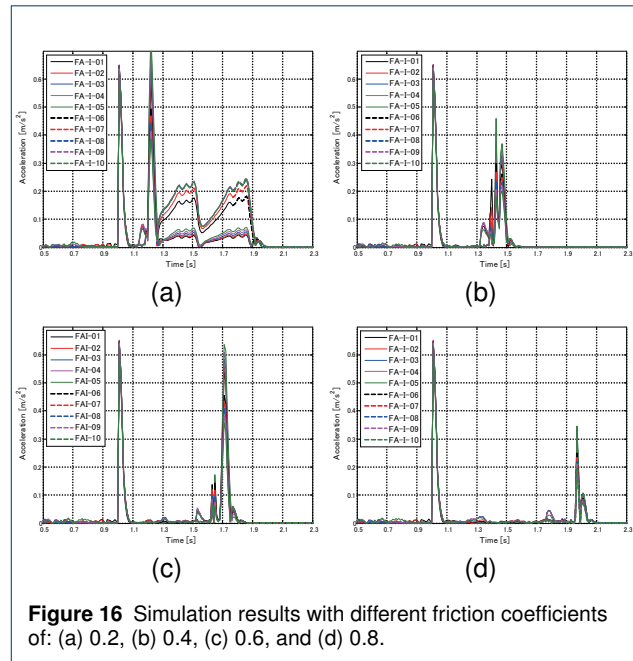
Figure 13 Acceleration responses using model with fingerprint and the original concaved phalanx at the locations of the receptors: (a) FA-I and (b) SA-I.



proportional to the friction coefficient. However, the time latency increased significantly from coefficient 0.2 to 0.6 and the increase becomes insignificant from coefficient 0.6 to 0.8. This suggests us that if we want to achieve a stable grasping or manipulation, we should increase the friction coefficient as much as possible. On the other hand, time latency has a limitation and we cannot have an arbitrary time latency for adjustment. From Fig. 16, we also found that large vibrations happened after overall slippage when small friction coefficient (0.2) was used. The middle peaks, which indicate the 3/4 overall slippage, disappeared and the peak magnitudes become smaller when large coefficient (0.8) was used (Fig. 16d). The reason to these behaviors is unclear in this moment and it needs further investigation.

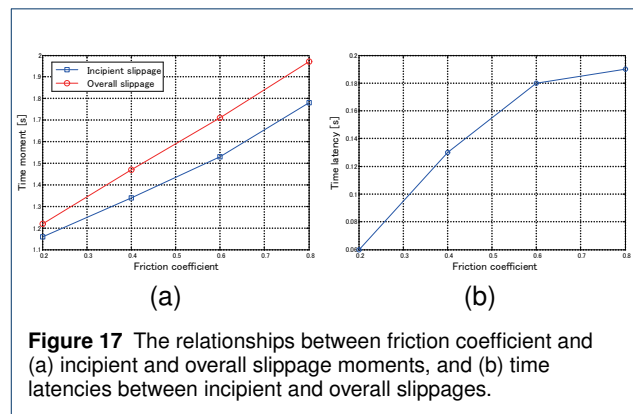
Experimental validation

An artificial fingertip was constructed to validate our findings. The fingertip has two soft layers made from polyurethane rubber and silicone. The inner layer mimicking the subcutaneous tissue was made from polyurethane rubber (Hitohada human skin gel, www.exseal.co.jp) with hardness zero. The outer layer mimicking the skin was made from transparent silicone rubber (Smooth-on Dragon Skin 30, www.smooth-on.com). The distal phalanx (Fig. 18a) was 3D printed with the same geometry as proposed in the FE model, and inserted into the first set of molds



which has the same geometry as the soft tissue. Then, polyurethane rubber resin was poured into the mold. After the soft tissue was cured, it was removed from the first set of molds and inserted into the second set of molds, which has the same geometry as the skin, to cast the skin layer by pouring silicone into the molds. The completed artificial fingertip is shown in Fig. 18b.

The experimental setup of pushing-and-sliding is shown in Fig. 19. The fingertip was rigidly fixed to the vertical linear stage (Suruga Seiki KXL06100-C2-F) via a rotary positioning stage. The vertically movable linear stage was then fixed to a horizontally movable linear stage. Both stages allow the fingertip to move in X and Z directions. The linear stages are capable of moving up to a speed of 50 mm/s. The linear stages were connected to a computer and controlled through LabView®. During experiments, the fingertip was pushed and slid against a transparent acrylic sheet, and a



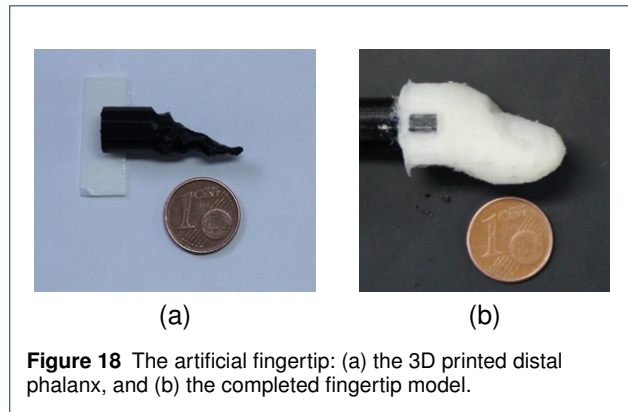


Figure 18 The artificial fingertip: (a) the 3D printed distal phalanx, and (b) the completed fingertip model.

Logitech HD Pro webcam was set underneath the acrylic sheet to capture the fingertip motions. The frame rate of the camera was set to 30 fps. The fingertip was initially moved in X direction to obtain an indentation of 2 mm and then slid on the acrylic sheet for 10 mm with a velocity of 5 mm/s. The video was later analyzed using MATLAB[®].

Figure 20 shows a few frames from the captured video. The green crosses in Fig. 20a indicate the tracked features of the markers on the contact area, and white lines shown in the rest of the figures indicate the displacements of the markers. We can see that a few peripheral points started to move prior to the center points in the moment of incipient slippage (Fig. 20b). After incipient slippage, movements spread from periphery to center before overall slippage (Fig. 20c). At the end of the experiment (Fig. 20d), it is very clear that the peripheral points obtained much larger displacements comparing with the points in the center area. This is consistent with the simulation results.

Conclusions

To study human perception of slippage and improve the development of human-like tactile sensor, FE models of an human fingertip were proposed based on MR image data. 3D FE model consists of layered structures were used to

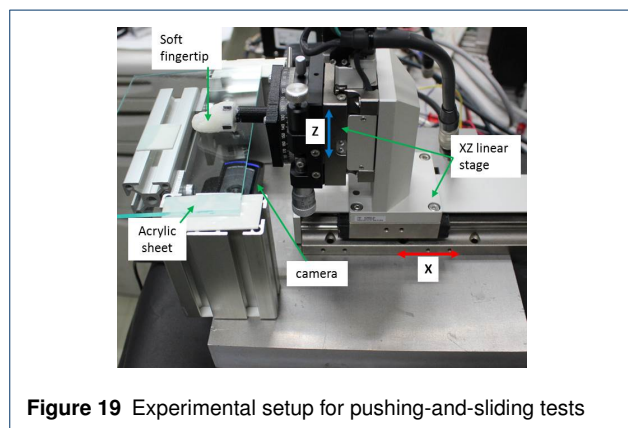


Figure 19 Experimental setup for pushing-and-sliding tests

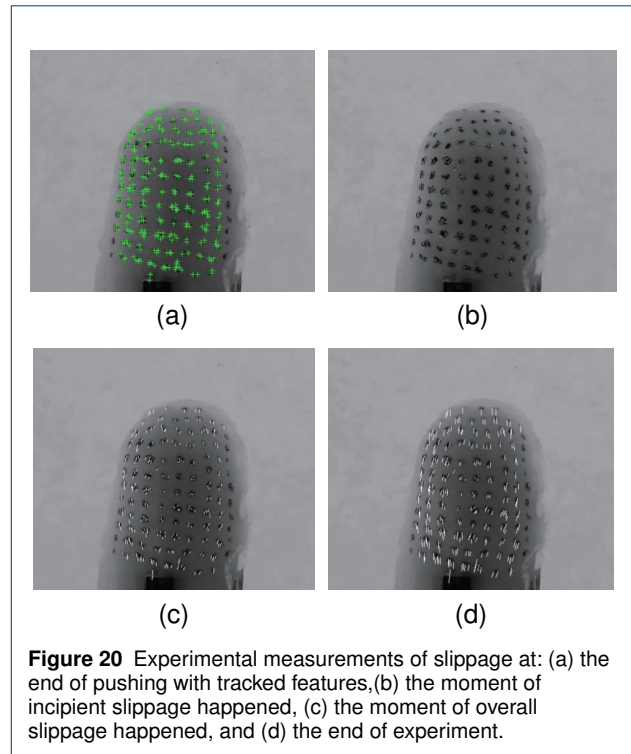


Figure 20 Experimental measurements of slippage at: (a) the end of pushing with tracked features, (b) the moment of incipient slippage happened, (c) the moment of overall slippage happened, and (d) the end of experiment.

simulate the macro behaviors during a pushing-and-sliding motion. According to simulation results, we found that the incipient slippage appeared firstly in the peripheral contact area and then spread from the peripheral area towards the center contact area until the overall slippage. Simulated acceleration data on the skin and soft tissue surfaces clearly showed the moments of incipient and overall slippages. Simulated stress data showed stress concentration at the concave area of the distal phalanx but did not provide any useful sign for the recognition of incipient and overall slippages.

To locate the four types of mechanoreceptors inside fingertip, 2D FE model consists of detailed micro-structures of the intermediate and limiting ridges was proposed. Through simulations, we found that the acceleration signals at the locations of mechanoreceptors clearly shows the moments of incipient and overall slippages but the SED signal does not provide useful information for detecting slippage. Acceleration responses at the locations of type FA-I and SA-I receptors are more pronounced comparing to the type FA-II and SA-II receptors.

The effect of distal phalanx was studied by comparing three different phalanx geometries: the original concave, the flattened, and the scaled phalanges. We found that the flattened and scaled phalanges advanced the incipient slippage and postponed the overall slippage, and therefore result in longer time latencies comparing to the original concave phalanx. However, only the original concave phalanx provides information of 3/4 overall slippage. The fin-

gerprint effect was also studied by modeling the fingerprint as a set of continuous ripples. Simulation results show that the fingerprint introduced obvious noise in acceleration signal and buried the indication signals of incipient and overall slippages. Finally, the effect of friction coefficient on slippage was investigated and we found that slippage moment is linearly proportional to the friction coefficient but the time latency has a limit during the increasing of friction coefficient.

An artificial fingertip mimicking the human fingertip was constructed using 3D printed phalanx and two layers of soft materials. Pushing-and-sliding tests were performed. The tracked motion of markers on skin surface was compared with simulation results and agreements were achieved.

In the future, different geometry modelings of fingerprints will be investigated and further study of fingerprint effects will be carried out. The moment of 3/4 overall slippage is worthy of further investigation using a high-accuracy geometry of distal phalanx. Tactile sensor having fingertip geometry and accelerometers embedded at locations of mechanoreceptors will be developed to further validate the findings in this paper.

Competing interests

The authors declare that they have no competing interests.

Author's contributions

WZ carried out all the simulations and drafted most of the manuscript except the section of experimental validation which was drafted by DSC. DSC also constructed the artificial fingertip model and performed the pushing-and-sliding tests. SH conceived the study and advised its progress. All authors read and approved the manuscript.

Acknowledgements

This work was supported by in part by MEXT-Supported Program for the Strategic Research Foundation at Private Universities (2013-2017) and in part by MEXT KAKENHI 26860404, JSPS, Japan.

Author details

All authors are with the Department of Robotics, Ritsumeikan University, Kusatsu, Shiga 525-8577, Japan {wangzk at fc, gr0120pr at ed, hirai at se}. ritsumei.ac.jp.

References

- Johansson, R.S., Westling, G.: Signals in tactile afferents from the fingers eliciting adaptive motor responses during precision grip. *Experimental Brain Research* **66**, 141–154 (1987)
- Ho, V.A., Hirai, S.: A novel model for assessing sliding mechanics and tactile sensation of human-like fingertips during slip action. *Robotics and Autonomous Systems* **63**, 253–267 (2015)
- Johansson, R.S., Vallbo, A.B.: Tactile sensory coding in the glabrous skin of the human hand. *Trends in Neurosciences* **6**, 27–32 (1983)
- Johansson, R.S., Flanagan, R.: Coding and use of tactile signals from the fingertips in object manipulation tasks. *Nature Reviews Neuroscience* **10**, 345–359 (2009)
- Phillips, J.R., Johnson, K.O.: Tactile spatial resolution. ii. neural representation of bars, edges, and gratings in monkey primary afferents. *Journal of Neurophysiology* **46**, 1192–1203 (1981)
- Phillips, J.R., Johnson, K.O.: Tactile spatial resolution. iii. a continuum mechanics model of skin predicting mechanoreceptor responses to bars, edges, and gratings. *Journal of Neurophysiology* **46**, 1204–1225 (1981)
- Srinivasan, M.A.: Surface deflection of primate fingertip under line load. *Journal of Biomechanics* **22**, 343–349 (1989)
- Srinivasan, M.A., Dandekar, K.: An investigation of the mechanics of tactile sense using two-dimensional models of the primate fingertip. *Journal of Biomechanical Engineering* **118**, 48–55 (1996)
- Lesniak, D.R., Gerling, G.J.: Predicting sa-i mechanoreceptor spike times with a skin-neuron model. *Mathematical Biosciences* **220**, 15–23 (2009)
- Dandekar, K., Raju, B.I., Srinivasan, M.A.: 3-d finite-element models of human and monkey fingertips to investigate the mechanics of tactile sense. *Journal of Biomechanical Engineering* **125**, 682–691 (2003)
- Wagner, M.B., Gerling, G.J., Scanlon, J.: Validation of a 3-d finite element human fingerpad model composed of anatomically accurate tissue layers. In: *Symposium on Haptic Interfaces for Virtual Environment and Teleoperator Systems*, pp. 101–105 (2008). IEEE
- Gerling, G.J., Rivest, I.I., Lesniak, D.R., Scanlon, J.R., Wan, L.: Validating a population model of tactile mechanotransduction of slowly adapting type i afferents at levels of skin mechanics, single-unit response and psychophysics. *IEEE Transactions on Haptics* **7**, 216–228 (2014)
- Johansson, R.S., Westling, G.: Roles of glabrous skin receptors and sensorimotor memory in automatic control of precision grip when lifting rougher or more slippery objects. *Experimental Brain Research* **56**, 550–564 (1984)
- Howe, R.D., Cutkosky, M.R.: Sensing skin acceleration for slip and texture perception. *IEEE Int. Conf. Robotics Automation* **1**, 145–150 (1989)
- Tremblay, M.R., Cutkosky, M.R.: Estimating friction using incipient slip sensing during a manipulation task. *IEEE Int. Conf. Robotics Automation* **1**, 429–434 (1993)
- Son, J.S., Monteverde, E.A., Howe, R.D.: A tactile sensor for localizing transient events in manipulation. *IEEE Int. Conf. Robotics Automation* **1**, 471–476 (1994)
- Canepa, G., Petrigliano, R., Campanella, M., Rossi, D.D.: Detection of incipient object slippage by skin-like sensing and neural network processing. *IEEE Transactions on Systems, Man, and Cybernetics-PART B: Cybernetics* **3**, 348–356 (1998)
- Fujimoto, I., Yamada, Y., Morizono, T., Umetani, Y., Maeno, T.: Development of artificial finger skin to detect incipient slip for realization of static friction sensation. In: *Proc. IEEE Int. Conf. Multisensor Fusion and Integration for Intelligent Systems*, pp. 15–20 (2003). IEEE
- Tada, M., Kanade, K.: An imaging system of incipient slip for modeling how human perceives slip of a fingertip. In: *Proc. the 26th Annual Int. Conf. the IEEE EMBS*, pp. 2045–2048 (2004). IEEE
- William, H., Ibrahim, Y., Richardson, B.: A tactile sensor for localizing transient events in manipulation. *International Journal of Optomechatronics* **1**, 46–62 (2007)
- Chathuranga, D.S., Wang, Z., Ho, V.A., Mitani, A., Hirai, S.: A biomimetic soft fingertip applicable to haptic feedback systems for texture identification. In: *Proc. IEEE Int. Symposium on Haptic Audio-Visual Environments and Games*, pp. 29–33 (2013). IEEE
- Wang, Z., Ho, V.A., Morikawa, S., Hirai, S.: A 3d non-homogeneous fe model of human fingertip based on mri measurements. *IEEE Transactions on Instrumentation & Measurement* **61**, 3147–3157 (2012)
- Gerling, G.J., Thomas, G.W.: Fingerprint lines may not directly affect sa-i mechanoreceptor response. *Somatosensory and Motor Research* **25**, 61–76 (2008)
- Maeno, T., Kobayashi, K., Yamazaki, N.: Relationship between the structure of human finger tissue and the location of tactile receptors. *JSM International Journal, Series C* **41**, 94–100 (1998)
- Scheibert, J., Leurent, S., Prevost, A., Debregeas, G.: The role of fingerprints in the coding of tactile information probed with a biomimetic sensor. *Science* **323**, 1503–1506 (2009)